Macro-Elements for Efficient FEM Simulation of Small Geometric Features in Waveguide Components

Yu Zhu, *Student Member, IEEE,* and Andreas C. Cangellaris, *Fellow, IEEE*

***Abstract*—This paper introduces a novel class of specially constructed elements aimed at the expedient finite-element modeling of waveguide components containing fine geometric/material features such as dielectric and conducting posts. Instead of utilizing a very fine grid to resolve such fine features, special elements are constructed that capture accurately the electromagnetic properties of the fine features. Since the size of these macro-elements is commensurate with the size of the elements of the grid used to discretize the volume in which the fine features are embedded, their use results in significant reduction in the number of unknowns in the finite-element approximation of the electromagnetic problem without sacrificing solution accuracy. The numerical implementation and effectiveness of the proposed macro-elements are demonstrated through several numerical experiments.**

***Index Terms*—Finite-element method, macro-element, model order reduction.**

I. Introduction

CONDUCTING and dielectric posts of small size are utilized extensively in the design of waveguide passive components [1], [2]. Typically, the cross sections of such posts are much smaller than the guide wavelength at the operating frequency of interest. Therefore, when finite methods are used for the analysis of such components, a very fine grid is required in the vicinity of the post in order to model accurately its impact on the electromagnetic performance of the component. This results in a significant increase in the number of degrees of freedom in the discrete problem and penalizes simulation efficiency.

In this paper, a new methodology is proposed for the modeling of fine material and geometry features inside waveguides. The basic idea behind this new method is the development of special elements that enclose the small feature of interest and, through a properly constructed transfer function, capture accurately the electromagnetic behavior of the small feature by describing the relationship between tangential electric and magnetic fields on the surface of the small feature domain. These special elements are called *macro-elements* [3], and their transfer function matrix representation is frequency-dependent and generated in such a way that the macro-elements can be used with any one of several popular finite methods or integral equation methods. We will refer to such a transfer function matrix as a *generalized impedance matrix* (GIM).

The incorporation of the macro-elements into the global electromagnetic solver is effected through the matching of the tangential electric and magnetic fields on the boundary shared by the macro-elements and their exterior regions. Instead of imposing this boundary condition one element at a time, the fields on the boundary could be expanded using global basis functions. For the purposes of this paper, we will refer to such global basis functions as *generalized modes*. Compared with the element-by-element imposition, this method allows for a different mesh to be used inside and outside the macro-elements, and thus eliminates the need for the meshes interior and exterior to their boundary to coincide. Another advantage is that the number of generalized modes considered is, usually, much smaller than that of the elements on the boundary of the macro-element. Thus, the transfer function matrices that describe the macro-elements are of small size. The choice of the generalized modes depends on the shape of the small-feature domain. Although a separable surface, such as a sphere, might be appealing at first sight for use as the macro-element boundary, generality and mesh generation simplicity make the use of a rectangular box a better choice. Then, orthonormal polynomial functions are the most convenient choice for the generalized modes on the macro-element rectangular boundaries.

To conclude this introductory summary of the proposed idea of the macro-element, we mention that the frequency dependence of its GIM suggests that a different transfer function matrix will need to be constructed for each different frequency over the bandwidth of interest. We will show that this apparent inconvenience can be handled by casting the elements of the GIM in closed form. In particular, our development of the transfer function matrix utilizes model order reduction techniques [7]–[9] to construct a broadband transfer function matrix in a computationally efficient manner.

In the first part of this paper, the methodology for the development of the macro-elements is presented. Next, the incorporation of the generated macro-elements in a finite-element model of the structure that includes the features described in terms of macro-elements is discussed. This paper concludes with a series of numerical examples that demonstrate the validity of the proposed macro-element concept and highlight the reduction in computational complexity resulting from their implementation.

Manuscript received March 3, 2000; revised August 21, 2000. This work was supported by the Motorola Center for Communications, College of Engineering, University of Illinois at Urbana-Champaign.

The authors are with the Department of Electrical and Computer Engineering, University of Illinois at Urbana-Champaign, Urbana, IL 61801 USA (e-mail: cangella@uiuc.edu).

Publisher Item Identifier S 0018-9480(00)10713-6.

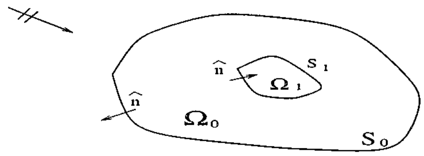

Fig. 1. The domain Ω_1 encloses a small feature in the FEM region Ω_0.

II. Development of the Macro-Elements

For the purposes of this paper, it is assumed that the finite-element method (FEM) is used for the discretization of the electromagnetic boundary value problem of interest.

Consider a source-free region $\Omega_0 + \Omega_1$, as shown in Fig. 1. This region is bounded by surface S_0, which is the outermost surface of the computational domain. Inside Ω_0, there is a small feature domain Ω_1, which is surrounded by the boundary S_1. More specifically, the term *small feature* is used in this paper to refer to material or geometry features of cross-sectional size comparable to the size of the elements used for the discretization of the domain Ω_0. The electric field $\vec{E}$ in Ω_0 obeys the vector wave equation [6]

$$\nabla \times \frac{1}{\mu} \nabla \times \vec{E} - \omega^2 \epsilon \vec{E} = 0 \tag{1}$$

where μ and ϵ are the permeability and permittivity, respectively. Multiplying (1) with an arbitrary weighting function $\vec{F}$ and integrating over the computational domain Ω_0, the weak form of (1) is obtained

$$\int_{\Omega_0} \left(\nabla \times \vec{F} \cdot \frac{1}{\mu} \nabla \times \vec{E} - \omega^2 \vec{F} \cdot \epsilon \vec{E} \right) dv \\ - j\omega \oint_{S_0 + S_1} \hat{n} \times \vec{H} \cdot \vec{F}\, ds = 0. \tag{2}$$

The corresponding matrix form of the finite-element approximation obtained from (1) is

$$\left(S_{\Omega_0} - \omega^2 T_{\Omega_0} \right) \vec{e} = j\omega \oint_{S_0+S_1} \hat{n} \times \vec{H} \cdot \vec{F}\, ds \tag{3}$$

where $\vec{e}$ is the expansion coefficients for $\vec{E}$

$$S_{\Omega_0\, ij} = \int_{\Omega_0} \nabla \times \vec{F}_i \cdot \frac{1}{\mu} \nabla \times \vec{F}_j\, dv, \quad T_{\Omega_0\, ij} = \int_{\Omega_0} \vec{F}_i \cdot \epsilon \vec{F}_j\, dv \tag{4}$$

and the right-hand side of (3) is understood as the matrix form of the forcing term.

Clearly, the domain Ω_1 is not included in the FEM formulation. Thus, there is no need for the use of a fine grid in the neighborhood of the small feature domain Ω_1. Instead, the impact of the material/geometry characteristics inside Ω_1 will be taken into account through the surface integral term over S_1 in (2). The way this is done using the concept of macro-elements is explained next.

The development begins by considering Maxwell's equations in the Laplace domain inside Ω_1 [3]

$$\nabla \times \vec{E} = -s\vec{B} \\ \nabla \times \left(\frac{\vec{B}}{\mu} \right) = s\,\epsilon\,\vec{E} + \sigma \vec{E} \tag{5}$$

where $s = j\omega$. The semidiscrete form of the two curl equations is obtained through the discretization of the domain Ω_1 and the expansion of $\vec{E}$ and $\vec{B}$ in their appropriate basis function spaces. More specifically, vector basis functions will be used. $\vec{E}$ is expanded in the tangentially continuous vector space (Whitney1-form) W_e [5], while $\vec{B}$ is in the normally continuous vector space (Whitney2-form) W_f [4].

Let $\vec{w}_e$ denote the basis functions in W_e and $\vec{w}_f$ denote the basis functions in W_f. Application of Galerkin's method, where the curl equations (5) are multiplied by $\vec{w}_f$ and $\vec{w}_e$, respectively, and integrated over the domain Ω_1, yields

$$\int_{\Omega_1} \nabla \times \vec{E} \cdot \frac{1}{\mu} \vec{w}_f\, dv \\ = -s \int_{\Omega_1} \vec{w}_f \cdot \frac{1}{\mu} \vec{B}\, dv \\ \cdot \int_{\Omega_1} \nabla \times \vec{w}_e \cdot \frac{1}{\mu} \vec{B}\, dv + \oint_{S_1} \hat{n} \times \vec{H} \cdot \vec{w}_e\, ds \\ = s \int_{\Omega_1} \vec{w}_e \cdot \epsilon \vec{E}\, dv + \int_{\Omega_1} \vec{w}_e \cdot \sigma \vec{E}\, dv \tag{6}$$

where unit normal $\hat{n}$ points into Ω_1. From these equations, the matrix form of the FEM approximation is obtained

$$\begin{pmatrix} 0 & D \\ -D^T & S \end{pmatrix} \begin{pmatrix} \vec{b} \\ \vec{e} \end{pmatrix} = -s \begin{pmatrix} P_b & 0 \\ 0 & P_e \end{pmatrix} \begin{pmatrix} \vec{b} \\ \vec{e} \end{pmatrix} + \begin{pmatrix} 0 \\ B \end{pmatrix} \tag{7}$$

where $\vec{e}$ and $\vec{b}$ are expansion coefficients for $\vec{E}$ and $\vec{B}$, respectively, and

$$D_{ij} = \int_{\Omega_1} \nabla \times \vec{w}_{e,\,i} \cdot \frac{1}{\mu} \vec{w}_{f,\,j}\, dv \\ S_{ij} = \int_{\Omega_1} \vec{w}_{e,\,i} \cdot \sigma \vec{w}_{e,\,j}\, dv \\ P_{b\,ij} = \int_{\Omega_1} \vec{w}_{f,\,i} \cdot \frac{1}{\mu} \vec{w}_{f,\,j}\, dv \\ P_{e\,ij} = \int_{\Omega_1} \vec{w}_{e,\,i} \cdot \epsilon \vec{w}_{e,\,j}\, dv \\ B_i = \oint_{S_1} \hat{n} \times \vec{H} \cdot \vec{w}_{e,\,i}\, ds. \tag{8}$$

At this point, it is worth noting that the finite-element formulation of the electromagnetic problem given in (7) and (8) is equivalent to the more traditional formulation associated with the weak form (3). This equivalence stems from the special relationship between Whitney-1 form (W_e) and Whitney-2 form (W_f) as pointed out in [4]

$$\nabla \times W_e^{p+1} \subset W_f^p. \tag{9}$$

In words, this equation states that the curl of the $(p+1)$th order Whitney-1 form belongs to the pth order Whitney-2 form. From this relationship, it can be shown (through some matrix manipulation) that

$$D^T P_b{}^{-1} D = S_{\Omega_1} \tag{10}$$

where

$$S_{\Omega_1,\,ij} = \int_{\Omega_1} \nabla \times \vec{w}_{e,\,i} \cdot \frac{1}{\mu} \nabla \times \vec{w}_{e,\,j}\, dv. \tag{11}$$

Thus, (7) can be reduced to the form of (3) through elimination of the magnetic field coefficient vector $\vec{b}$.

Note that the matrix B in (7) can be used to impose boundary conditions on the surface of the domain Ω_1. More specifically, let us assume that a natural boundary condition is imposed on S_1. Instead of expanding $\hat{n} \times \vec{H}$ using edge basis functions $\vec{w}_e$, an orthonormal set of global vector functions $\vec{f}_n(S_1)$ on the surface S_1 of domain Ω_1 is used for the expansion of the tangential magnetic field

$$\hat{n} \times \vec{H} = \sum_{n=0}^{p-1} i_n \vec{f}_n(S_1) \tag{12}$$

where i_n is the expansion coefficient for the nth function. As discussed in the introduction, the two primary attributes of this choice of expansion functions are the decoupling of the interior and exterior finite-element grids and the compact size of the resulting GIM. With Ω_1 taken to be a rectangular box, the bounding surfaces are of planar rectangular shapes. On these surfaces, orthonormal Legendre polynomials are used as the expansion functions $\vec{f}_n(S_1)$.

In compact form, the discrete system of (7) is given by

$$(G + sC)\, X = B\, I(s) \tag{13}$$

where

$$G = \begin{pmatrix} 0 & D \\ -D^T & S \end{pmatrix}, \qquad C = \begin{pmatrix} P_b & 0 \\ 0 & P_e \end{pmatrix}$$

$$B_{ij} = \oint_{S_1} \vec{w}_{e,\,i} \cdot \vec{f}_j(S_1)\, ds, \qquad X = \begin{pmatrix} \vec{b} \\ \vec{e} \end{pmatrix} \tag{14}$$

and $I(s)$ contains the coefficients i_n in the expansion of $\hat{n} \times \vec{H}$.

From the vector of unknowns X, the desired outputs are the expansion coefficients for the tangential electric fields on S_1. Let

$$\vec{E}_t = \sum_{n=0}^{p-1} v_n \vec{f}_n(S_1) \tag{15}$$

be the expansion of these tangential electric field on S_1 in terms of the vector global basis function $\vec{f}_n(S_1)$, where v_n are the expansion coefficients. These coefficients can be extracted by multiplying X with the conjugate transpose of B. More specifically, let $V(s)$ denote the vector containing the expansion coefficients v_n. It is then

$$V(s) = B^H\, (G + s\; C)^{-1} B\, I(s) = Z(s) I(s). \tag{16}$$

This last equation defines the desired GIM that captures the electromagnetic properties of the structure inside the volume Ω_1 through a global impedance relationship between the tangential magnetic and electric fields on S_1. It is shown in [10] that the skew symmetry of G, the positive definiteness of C, and the nonnegative definiteness of S ensure that the semidiscrete system resulting from the spatial discretization of Maxwell's equations maintains the passive character of the original continuous electromagnetic system. It is this GIM that constitutes the proposed macro-element. The way it is incorporated in the finite-element solution of the exterior domain Ω_0 will be discussed in the next section.

III. Broadband Closed-Form Expression of the GIM

Clearly, the GIM of (16) is a function of frequency. Thus, once generated, it can be used for the solution of the electromagnetic problem in Ω_0 at any frequency of interest. A more convenient form of the matrix $B^H(G + sC)^{-1}B$ can be obtained through an eigen-decomposition of the matrix $C^{-1}G$. This would lead to a matrix form where the matrix $(G + sC)^{-1}$ has been replaced by the inverse of a diagonal matrix $(\Lambda + sU)$, where Λ is the diagonal matrix containing the eigenvalues of $C^{-1}G$ and U is the identity matrix. Consequently, its inversion is trivial, and a closed-form representation of the elements of the GIM becomes possible in a pole-residue form. The order of this pole-residue form is equal to the number of degrees of freedom in the FEM discretization of Ω_1. Since the discretization of Ω_1 is driven by the need to resolve accurately the fine features inside this volume, the number of degrees of freedom is often much higher than that needed for a transfer impedance description of the electromagnetic properties of the structure inside the volume as seen from its exterior. This suggests the development of a reduced-order model of the transfer impedance matrix using, for example, the passive model order reduction algorithm PRIMA [8].

The model order reduction process in PRIMA is based on the congruence transformation

$$X = W\, \tilde{X} \tag{17}$$

where $\tilde{X}$ is the reduced state vector. Its length q is much smaller that the length N of the original vector X. The transformation matrix W is generated using the Arnoldi algorithm and is chosen to be orthonormal bases for the block Krylov subspace $Kr(A,\, R,\, q)$ [8]

$$\begin{aligned} Kr(A,\, R,\, q) = colsp[&R,\, AR,\, A^2R,\, \ldots,\, A^{\hat{n}-1}R, \\ &A^{\hat{n}}r_0,\, A^{\hat{n}}r_1,\, \ldots,\, A^{\hat{n}}r_l] \end{aligned} \tag{18}$$

where $A = -(G+s_0C)^{-1}C$, $R = (G+s_0C)^{-1}\, B$, $\hat{n} = \lfloor q/p \rfloor$, $l = q - \hat{n}p$, and s_0 is properly selected complex expansion frequency.

Substitution of (17) into (13) and multiplication on the left by W^H yields

$$(W^H\, GW + sW^H\, CW)\tilde{X} = W^H\, B\, I(s). \tag{19}$$

Thus the transfer function matrix of the reduced system is given by

$$\tilde{Z}(s) = \tilde{B}^H\, (\tilde{G} + s\tilde{C})^{-1}\tilde{B} \tag{20}$$

where the matrices in the reduced-order system are

$$\tilde{G} = W^H\, GW, \quad \tilde{C} = W^H\, CW, \quad \tilde{B} = W^H B. \tag{21}$$

A more convenient form of (20) is obtained through the eigen-decomposition $\tilde{A} = \tilde{C}^{-1}\tilde{G}$ [3]

$$\tilde{A} = Q\Lambda_q Q^{-1} \tag{22}$$

where $\Lambda_q = \mathrm{diag}(\lambda_1,\, \lambda_2,\, \ldots\, \lambda_q)$. Substitution of (22) in (20) yields

$$\tilde{Z}(s) = \tilde{B}^H Q\, (sU + \Lambda_q)^{-1}\, Q^{-1}\, \tilde{C}^{-1}\tilde{B}. \tag{23}$$

Let $u^{(i)}$ denote the ith row vector of $\tilde{B}^H Q$ and $v^{(j)}$ the jth column vector of $Q^{-1}\tilde{C}^{-1}\tilde{B}$. Then, the (i, j)th element of the transfer impedance matrix assumes the pole-residue form

$$\tilde{Z}_{ij}(s) = \sum_{n=1}^{q} \frac{u_n^{(i)} \cdot v_n^{(j)}}{s + \lambda_n}. \tag{24}$$

It should be mentioned the main cost of the development of the reduced-order form of the macro-element GIM is the inversion of matrix $(G + s_0 C)$ that is required for the construction of $Kr(A, R, q)$. Since the volume of the small-feature domain is small, the cost is acceptable, especially in view of the fact that it yields a closed-form broadband expression for the GIM of the macro-element. The choice of the expansion frequency s_0 depends on the bandwidth of interest [7]. More specifically, if the maximum frequency of interest is $f_{\max}$, we set $s_0 = 2\pi f_{\max}$. The order q depends on the complexity of the structure inside the macro-element and its impact on the field variation with frequency. For the electrically small domains considered here, the order is less than ten.

This completes the development of the macro-element of the domain Ω_1 through the reduced-order pole-residue representation of its GIM. Its incorporation into the global FEM model is presented in the following section.

IV. Incorporation of Macro-Elements in the Global FEM Matrix

The integration of the proposed macro-element into the global FEM simulation is effected through the surface integral over S_1 in (3). On S_1

$$\begin{aligned} \hat{n} \times \vec{H} &= \left[\vec{f}_0, \vec{f}_1, \ldots, \vec{f}_{p-1}\right] \begin{bmatrix} i_0 \\ i_1 \\ \vdots \\ i_{p-1} \end{bmatrix} \\ &= \left[\vec{f}_0, \vec{f}_1, \ldots, \vec{f}_{p-1}\right] \tilde{Z}(s)^{-1} \begin{bmatrix} v_0 \\ v_1 \\ \vdots \\ v_{p-1} \end{bmatrix} \end{aligned} \tag{25}$$

where

$$v_i = \oint_{S_1} \vec{f}_i \cdot \vec{E}\, ds. \tag{26}$$

Substitution of (25) into the surface integral over S_1 in (3) yields

$$\begin{aligned} \oint_{S_1} \hat{n} \times \vec{H} \cdot \vec{F}\, ds &= \oint_{S_1} \vec{F} \cdot \left[\vec{f}_0, \vec{f}_1, \ldots, \vec{f}_{p-1}\right] ds \cdot \tilde{Z}(s)^{-1} \\ &\quad \cdot \oint_{S_1} \begin{bmatrix} \vec{f}_1 \\ \vec{f}_2 \\ \vdots \\ \vec{f}_{p-1} \end{bmatrix} \cdot \vec{E}\, ds \\ &= M\, \tilde{Z}(s)^{-1} M^T \vec{e} \end{aligned} \tag{27}$$

where M is an $N \times p$ matrix

$$M_{ij} = \oint_{S_1} \vec{F}_i \cdot \vec{f}_j\, ds. \tag{28}$$

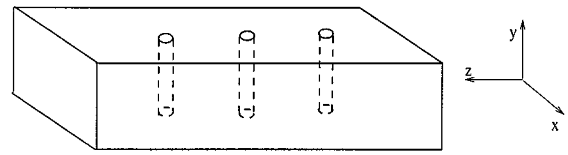

Fig. 2. Vertical posts inside a rectangular waveguide.

The matrix form in (27) will be added to the external global FEM system matrix to account for the electromagnetic effects of the small features.

To summarize, the basic idea discussed in this paper is the development of a macro-element description of a fine feature inside a domain, via the generation of the generalized impedance matrix (GIM) on the surface of small volume that encloses the fine feature. GIM provides a rigorous frequency-dependent relationship between the tangential electric and magnetic fields. The construction of the GIM was based on a finite-element formulation of the electromagnetic problem that is compatible with passive model order reduction techniques, and thus enables the direct development of broadband closed-form pole-residue representations of the frequency-dependent elements of GIM of order small enough to make its subsequent utilization in the external finite-element problem computationally efficient. It is emphasized that the incorporation of the macro-element into the finite-element formulation of the external problem is effected in a straightforward fashion through (27). Thus, once the GIM description of the macro-element has been obtained, the electromagnetic properties of the fine feature are rigorously described by it, and the integration of the macro-element into its environment depends solely on the footprint of the exterior grid on the surface of the macro-element.

V. Numerical Examples

The following numerical examples focus on the specific cases where thin vertical dielectric or conducting posts of constant cross section are present inside a rectangular waveguide, as shown in Fig. 2. It is assumed that the incident (excitation) mode is the TE_{10} mode. Due to the post orientation and geometry, only TE_{m0} modes are excited by their presence. Consequently, there is no field variation in the y direction, and a two-dimensional grid is needed for the numerical solution of this class of structures. All numerical studies focus on the calculation of the reflection and transmission coefficients for the dominant TE_{10} mode, caused by the presence of geometric or material discontinuities inside the waveguide.

We consider first the case of a single vertical metallic wire inside a rectangular waveguide. A FEM modeling of the structure requires an average grid size in the order of one-twentieth of the wavelength at the maximum frequency. The size of the wire is assumed to be comparable to the size of the FEM cell. A FEM cell is used to enclose a post, as shown in the figure. Without loss of generality, the cell is assumed to have a rectangular cross section. The region inside the cell around the thin wire is discretized using a finer grid, as shown in Fig. 3, for the purpose of developing the GIM for its macro-element description. The region outside the macro-element is discretized using a regular grid.

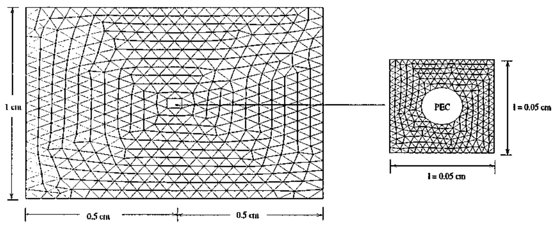

Fig. 3. Top view of the finite-element grid used for the discretization of the waveguide containing a single metallic post. The fine grid used in the interior of the rectangular macro-element that encloses the post is shown on the right.

Since the fields are $\hat{y}$ invariant, one-dimensional Legendre expansions on each of the four surfaces of the rectangular cell are sufficient. Furthermore, the small electrical size of the cell suggests that a zeroth-order Legendre polynomial expansion should be sufficient. Thus, on each side of the rectangular box that encloses the wire, tangential electric and magnetic fields are taken to be constant

$$\begin{aligned}\hat{n} \times \vec{H}_n &= i_n \frac{1}{\sqrt{l}} \hat{y} \\ \vec{E}_n &= v_n \frac{1}{\sqrt{l}} \hat{y}.\end{aligned} \tag{29}$$

Consequently, the GIM representation of the macro-element description of the thin wire assumes the simple form

$$\begin{bmatrix} v_1 \\ v_2 \\ v_3 \\ v_4 \end{bmatrix} = \tilde{Z}(s) \begin{bmatrix} i_1 \\ i_2 \\ i_3 \\ i_4 \end{bmatrix}. \tag{30}$$

The aforementioned impedance relationship is incorporated in the external finite-element model of the waveguide through the surface integral term associated with the macro-element boundary as described by (27). More specifically, since the cell used in this example is itself an element of the external mesh, the relevant degrees of freedom are the electric field nodes at the four corners and the tangential magnetic fields along the four sides (see Fig. 4). Thus, the matrix M in (27) assumes the simple form

$$M = \frac{\sqrt{l}}{2} \begin{bmatrix} 1 & & & 1 \\ 1 & 1 & & \\ & 1 & 1 & \\ & & 1 & 1 \end{bmatrix} \begin{array}{l} \leftarrow \text{node } \hat{1} \\ \leftarrow \text{node } \hat{2} \\ \leftarrow \text{node } \hat{3} \\ \leftarrow \text{node } \hat{4}. \end{array} \tag{31}$$

Finally, the matrix $M\tilde{Z}(s)^{-1}M^T$ is added to the global FEM system matrix.

Fig. 5 depicts the magnitude of the reflection coefficients for a single cylindrical metallic wire versus frequency and for three different values of its radius. The largest value of the wire radius is taken to be 0.015 cm. The waveguide is air-filled of width (along x) of 1 cm. As indicated in Fig. 4, the cell that includes the wire is square of side 0.05 cm. This value represents also the average size of the elements in the finite-element grid used for the discretization of the waveguide.

For each radius, the calculated reflection coefficient is compared with the analytic solution [1], depicted in the figure (using $\circ$ for $r = 0.005$ cm, $\times$ for $r = 0.01$ cm, and $\diamond$ for $r = 0.015$ cm). In all cases, very good agreement is observed over the entire bandwidth. Clearly, the wire radius has a significant effect on the reflection coefficient and cannot be ignored. The approximation of the thin circular post as a wire of zero thickness can lead to significant error in the solution.

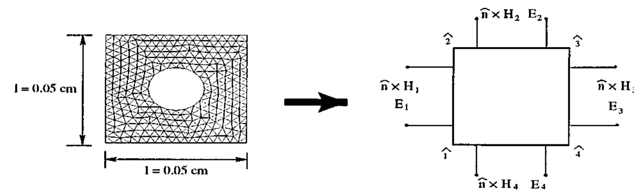

Fig. 4. Development of the macro-element for the vertical post.

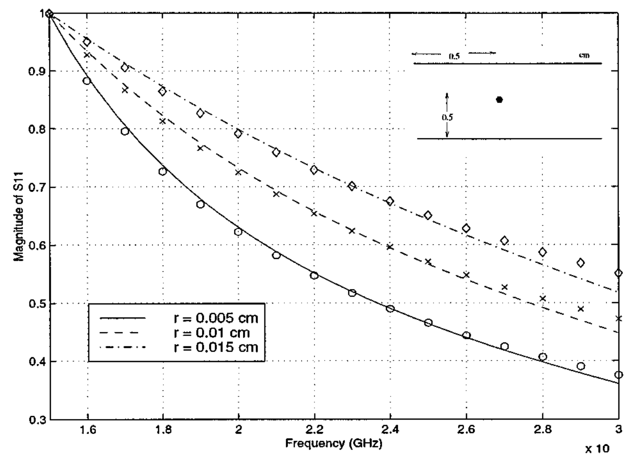

Fig. 5. Reflection coefficient of a single metallic post placed vertically inside a rectangular waveguide.

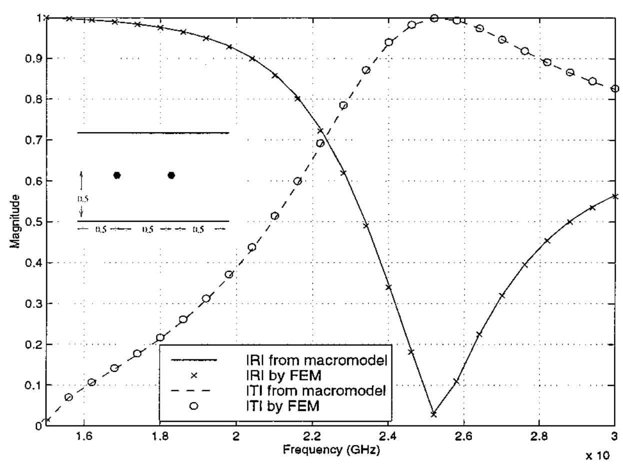

Fig. 6. Reflection and transmission coefficients for two metallic posts placed vertically inside a rectangular waveguide.

The second numerical example deals with the case where two thin metallic posts are present inside the waveguide of example 1. The two posts are identical, and thus the same macro-element description is used for each one of them. Fig. 6 depicts the magnitude versus frequency for the reflection and transmission coefficients for the case where the radius of each post is 0.01 cm. The results obtained using the macro-element formulation are in very good agreement with those obtained using a brute-force FEM solution with a much finer grid, capable of modeling accurately the finite radius of the two posts.

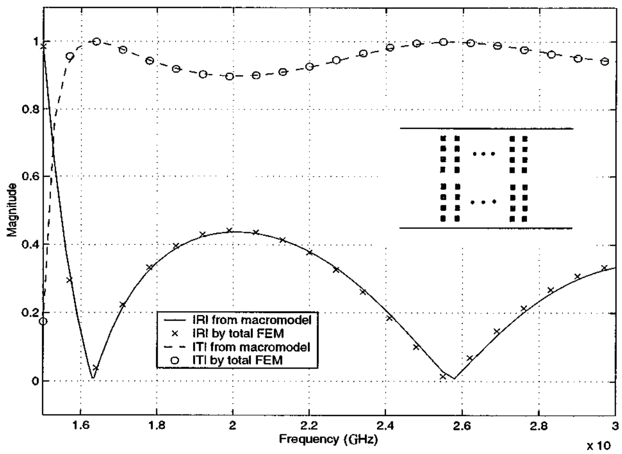

Fig. 7. Reflection and transmission coefficients for an 8 × 10 array of dielectric posts with $\epsilon_r = 20$ placed inside a rectangular waveguide.

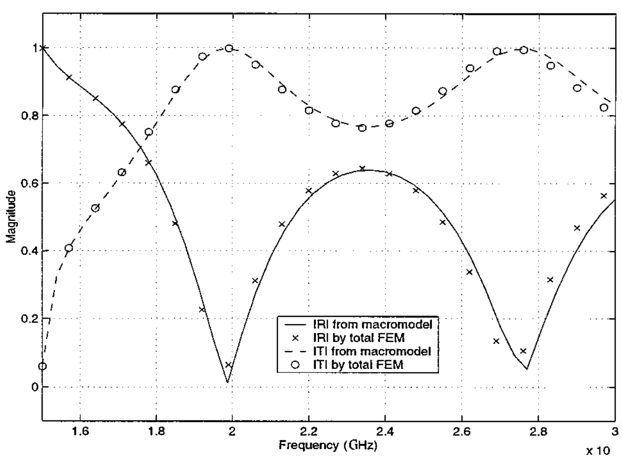

Fig. 8. Reflection and transmission coefficients for an 8 × 10 array of dielectric posts with $\epsilon_r = 50$ placed inside a rectangular waveguide.

The final example considers the case of dielectric posts inserted in waveguides. More specifically, a finite array of 8 × 10 dielectric posts, with relative dielectric constant $\epsilon_r = 20$, is placed inside the waveguide. The average grid size of the global finite element mesh is 0.05 cm, while the cross section of each dielectric post is square of size 0.02 × 0.02 cm^2. The insert in Fig. 7 depicts the configuration of the array. The separation between adjacent columns of dielectric posts is 0.1 cm. Each one of the ten columns has eight posts, which split into two groups of four posts each. The separation between the two groups of four posts is 0.15 cm. In each group, the separation between adjacent posts is 0.1 cm; the separation of each group of four posts from the side waveguide walls is 0.125 cm.

Since all posts are identical, only a single macro-element needs to be generated to capture the electromagnetic properties of each post. As can been seen from Fig. 7, the reflection and transmission coefficients obtained using the macro-elements match those obtained using a fine-grid FEM model. Very good agreement is also obtained for the case where $\epsilon_r = 50$ (see Fig. 8). When use is made of the macro-element representation of each post, the number of unknowns in the global FEM model is equal to 960. If the macro-elements are not utilized, a much finer FEM grid is required. For the case of dielectric posts of relative dielectric constant of 50, the number of unknowns used in the fine grid is ~96 000, two orders of magnitude larger than that for the case when macro-elements are implemented.

VI. Concluding Remarks

A methodology has been proposed for the enhancement of the computational efficiency with which fine material and geometry features are modeled inside passive waveguide components using the method of finite elements. The emphasis is on features smaller in size than the average grid size required for the discretization of the global waveguide geometry. Metallic and dielectric posts and thin slots are typical examples of such fine structures. Instead of using a locally refined grid in the vicinity of the fine feature, the proposed methodology generates a transfer impedance matrix representation of the volume containing the fine feature. This matrix representation is called the generalized impedance matrix of the fine feature and provides a frequency-dependent impedance relationship between the tangential electric and magnetic fields over the surface that encloses the fine feature. Once generated, the GIM can be stamped directly in the finite-element matrix that describes the discretized electromagnetic problem of the global volume exterior to the volume enclosing the fine feature. Thus, such a GIM acts in effect as a macro-element description of the electromagnetic behavior of the fine feature.

The generated GIM description of the macro-elements is frequency dependent. In particular, a model order reduction methodology was introduced to cast each element of the GIM in a pole-residue form with the frequency as a parameter. In other words, each element of the GIM is available in a frequency-dependent closed-form expression. The maximum frequency of validity of the closed-form expression is dictated by the grid size of the finite-element mesh used to discretize the volume that contains the fine feature. The proposed macro-elements were used in the finite-element modeling of metallic and dielectric posts inside rectangular waveguides. Calculated results for reflection and transmission coefficients were in excellent agreement with those obtained either from analytic solution or brute-force finite-element modeling of these structures using very fine grids. Use of the macro-elements results in significant reduction in the number of unknowns required for the finite-element approximation of the geometries considered using grid refinement in the vicinity of the fine features. In addition to savings in memory and computational efficiency, the use of macro-elements facilitates finite-element grid generation. The idea is applicable to other finite methods (e.g., finite difference and finite volume methods).

The concept of the macro-element paves the way toward the systematic development of an electromagnetic response library for small features used frequently in the design of passive microwave components. This library of electromagnetic responses can be used in conjunction with the most common finite-element or finite-difference based electromagnetic solvers and can have a significant impact on reducing the modeling and discretization complexity of waveguide structures populated with a large number of fine-feature components.

REFERENCES

[1] R. Collin, *Field Theory of Guided Waves*. Oxford, U.K.: Oxford Univ. Press, 1991.

[2] P. G. Lia, T. Admas, Y. Leviatan, and J. Perini, "Multiple-post inductive obstacles in rectangular waveguide," *IEEE Trans. Microwave Theory Tech.*, vol. MTT-32, pp. 365–373, April 1984.

[3] A. Cangellaris, M. Celik, S. Pasha, and L. Zhao, "Electromagnetic model order reduction for system-level modeling," *IEEE Trans. Microwave Theory Tech.*, vol. 47, pp. 840–849, June 1999.

[4] A. Bossavit and I. Mayergoyz, "Edge-elements for scattering problems," *IEEE Trans. Magn.*, vol. 25, pp. 2816–2822, June 1999.

[5] J. P. Webb, "Hierarchal vector basis functions of arbitrary order for triangular and tetrahedral finite elements," *IEEE Trans. Antennas Propagat.*, vol. 4, pp. 1244–1253, Aug. 1999.

[6] J. F. Lee, "Tangential vector finite elements and their application to solving electromagnetic scattering problems," *Appl. Computat. Electromagn. Soc. Newsletter*, vol. 10, pp. 52–75, Mar. 1995.

[7] P. Feldmann and R. W. Freund, "Efficient linear circuit analysis by Pade approximation via the Lanczos process," *IEEE Trans. Computer-Aided Design*, vol. 14, pp. 639–649, May 1995.

[8] A. Odabasioglu, M. Celik, and L. T. Pileggi, "PRIMA: Passive reduced-order interconnect macromodeling algorithm," *IEEE Trans. Computer-Aided Design*, vol. 17, pp. 645–653, Aug. 1998.

[9] M. Zunoubi, K. C. Donepudi, J. M. Jin, and W. C. Chew, "Efficient time-domain and frequency-domain finite-element solution of Maxwell's equations using spectral Lanczos algorithms," *IEEE Trans. Microwave Theory Tech.*, vol. 46, pp. 1141–1149, Aug. 1998.

[10] A. C. Cangellaris and L. Zhao, "Passivity of discrete electromagnetic systems," in *Proc. 14th Annu. Rev. Progress Appl. Computational Electromagn.*, Monterey, CA, Mar. 1998, pp. 721–731.

Yu Zhu (S'00) received the B.S. degree from Nanjing University, China, in 1995 and the M.S. degree from The Ohio State University, Columbus, in 1998, both in electrical engineering. He is currently pursuing the Ph.D. degree in the Department of Electrical and Computer Engineering, University of Illinois at Urbana-Champaign.

He is a Graduate Research Assistant there. His research interests are in computational electromagnetics, finite-element method, and microwave engineering.

Andreas C. Cangellaris (M'86–SM'97–F'00) received the diploma from the Aristotle University of Thessaloniki, Greece, in 1981 and the M.S. and Ph.D. degrees from the University of California, Berkeley, in 1983 and 1985, respectively, all in electrical engineering.

From 1985 to 1987, he was a Senior Research Engineer in the Electronics Department of the General Motors Research Laboratories in Warren, MI. From 1987 to 1997, he was with the Department of Electrical and Computer Engineering, University of Arizona, Tucson, first as an Assistant Professor from 1987 to 1992 and then as an Associate Professor from 1992 to 1997. Since 1997, he has been a Professor of electrical and computer engineering at the University of Illinois at Urbana-Champaign. He is an author or coauthor of more than 120 papers in scientific journals and conference proceedings in the areas of computational electromagnetics, modeling and simulation of the electrical performance of high-speed interconnections, and electromagnetic analysis of packaging structures for high-speed electronics. In 1998, he was General Chair for the 8th Biennial Conference on Electromagnetic Field Computation (CEFC) and he is currently serving on the International Steering Committee for this conference.

Prof. Cangellaris is a member of the IEEE Antennas and Propagation Society, the IEEE Microwave Theory and Techniques Society, the IEEE Components, Packaging, and Manufacturing Technology Society, and the IEEE Electromagnetic Compatibility Society. He is a Cofounder of the IEEE Topical Meeting on Electrical Performance of Electronic Packaging. He is an Associate Editor for the IEEE TRANSACTIONS ON ADVANCED PACKAGING and the IEEE Press series on Electromagnetic Waves.